PCCP

Modeling of surface *vs.* bulk ionic conductivity in fixed charge membranes

Salvador Mafé,*[a] José A. Manzanares[a] and Patricio Ramirez[b]

[a] *Departament de Termodinàmica, Universitat de València, E-46100 Burjassot, Spain*
[b] *Departamento de Fisica Aplicada, Universidad Politécnica de Valencia, E-46022 Valencia, Spain. E-mail: smafe@uv.es*

Received 27th September 2002, Accepted 13th November 2002
First published as an Advance Article on the web 29th November 2002

A two-region model for describing the conductivity of porous fixed charge membranes is proposed. In the surface region, the conductivity is due to the mobile positive ions (counterions) around the negative fixed charges. In the pore center region, the conductive properties resemble those of the external electrolyte solution because the fixed charges are assumed to be effectively neutralized by the counterions in the surface region. Activation energies and surface diffusion coefficients are estimated by assuming that the counterion jump from a fixed charge group is the rate limiting process for surface transport. The barrier energy for this jump is calculated using a simple electrostatic model with two microscopic parameters, the sum of the counterion and fixed charge hydration radii and the local dielectric constant. The bulk conductivity is obtained from experimental data. The total membrane conductivity and the counterion transport number are then calculated as functions of the external solution concentration for several pore radii and membrane fixed charge concentrations. The results are compared with those given by the Donnan model for homogeneous membranes and by the numerical solution of a continuous model based on the Poisson–Boltzmann equation extended to finite size ions. The study of the membrane conductivity for a series of electrolytes allows to distinguish clearly between the mechanism characteristic of the bulk ionic conductivity and that of surface conductivity. The surface conductivity is found to be significant for narrow pores at low external solution concentrations.

Introduction

The interpretation of ionic equilibrium and transport in polymer fixed charge membranes (ion exchange membranes) has usually invoked the existence of two kinds of counterions:[1–8] those located close to the membrane fixed charges and those forming (together with their corresponding coions) the electroneutral salt taken by the membrane upon swelling. The latter ions distribute over regions where the influence of the membrane fixed charges is very small, and are thus supposed to exhibit properties similar to those of the external solution. Although such a distinction between counterions is not rigorously defined, it can contribute to a qualitative understanding of the physical mechanisms operating in fixed charge membranes. Therefore, when modeling the electrical properties of these membranes, theories have usually considered the membrane as composed of two or more conducting regions.[4–6,9,10]

We study here a model membrane composed by pores having two conducting regions. In the surface region the electric current is carried exclusively by the mobile positive ions (counterions) around the negative fixed charges attached to the pore boundaries. In the pore center region the conductive properties resemble those of the external electrolyte solution because the fixed charges are assumed to be effectively neutralized by the counterions in the surface region. This assumption could be appropriate for membranes with a high fixed charge concentration where the electrostatic potential variation from the surface to the center of the pore is confined to a thin solution layer.[11] Therefore, by surface conductivity we do not mean here that part of the membrane conductivity due to the electrodiffusion of mobile ions in the electric double layer close to a uniformly charged plane, as it is the case of the continuous models.[12,13] Instead, it is the counterion hopping between neighboring fixed charge groups that originates the surface conductivity in this model. Note also that the present approach is different to previous models[4,5] that consider the membrane as a heterogeneous system formed by two regions separated spatially, a gel phase containing the fixed charges together with the corresponding counterions, and a solution phase formed by volume inclusions of the electroneutral sorbed salt. Moreover, the Debye shielding characteristic of the continuum approaches[12] and the assumption of thermodynamic equilibrium between macroscopic phases characteristic of the Donnan formalism[1] are not invoked here.

Recent experimental studies[7,14,15] have shown that the three crucial factors for designing fixed charge membranes of higher conductivity are the electrostatic interactions between the counterions and the fixed charges, the relative sizes of mobile ions and membrane effective pores, and the membrane structural properties. The first two factors are addressed here. In particular, activation energies and diffusion coefficients for the surface conductivity are estimated using a simple microscopic model that considers the counterion displacement from a fixed charge group as the rate limiting process. The jump energetics is assumed to depend on the sum of the counterion and fixed charge hydration radii and the local dielectric constant for the water layer between these two electrical charges. The bulk conductivity is taken from experimental data. The total membrane conductivity and the counterion transport number are then obtained as a function of the solution concentration for pores having different radii and fixed charge concentrations. Calculations are intended to predict the qualitative trends and orders of magnitude of the two contributions to the total conductivity rather than to model quantitatively a

 DOI: 10.1039/b209438j

particular membrane. Finally, the study of the concentration dependence of the membrane conductivity for several electrolytes shows clearly the differences between the mechanism characteristic of the bulk ionic conductivity and the hopping mechanism characteristic of surface counterion conductivity. This mechanism should be important for narrow pores at low external solution concentrations. Our study is concerned mainly with synthetic polymer membranes, since many ionic channels in biological membranes have effective diameters comparable to the permeating ion size, and the assumptions of the present model are not valid for them.

Theoretical modeling of the conducting regions

The present approach makes use of previous concepts by Pourcelly *et al.*[16] and Eikerling *et al.*[11,17] although it incorporates also new ideas concerning the surface diffusion energetics and the definition of the membrane conductivity regions. Moreover, the Debye shielding characteristic of the continuum approaches[12] and the assumption of thermodynamic equilibrium between macroscopic phases characteristic of the Donnan formalism[1] are not invoked here, and the results obtained will be compared to those given by these models.

Fig. 1 shows a schematic view of the pore cross section. The negative fixed charges attached to the pore surface are surrounded by the mobile positive ions responsible for the surface conductivity on a layer roughly one hydrated counterion thick. The inner circle in Fig. 1 denotes the limit of the surface conduction zone, the pore center being filled by an electroneutral bulk solution. Then, the pore cross section area A_p is divided into a surface area A_s and a pore center area A_b. The respective area fractions are $f_s = A_s/A_p = 1 - f_b$ and $f_b = A_b/A_p = (1 - 2r_i/R)^2$, where r_i and R are the effective radius of the hydrated ion and the pore radius, respectively.

The model makes use of some simplifying assumptions. The division of the total membrane conductivity into surface and bulk contributions, though reasonable, constitutes a first idealization.[11] Also, the particular membrane topology (*e.g.* the pore size distribution) is ignored[17–19] since we assume that the whole membrane can be characterized by only one typical pore of uniform cross section. The surface conduction is analyzed on the basis of a simple electrostatic energy term that contains two microscopic parameters. Moreover, the electroosmotic contribution to the membrane conductivity[9,20] is ignored: surface conductivity occurs without net water transport (except for the counterion hydration water) and the bulk conductivity is assumed to be the same of an equivalent aqueous solution of the corresponding salt. Finally, ion pairing between the counterion and the fixed charge group is disregarded (this effect might be relevant for divalent counterions[21] and low water content membranes[22]). Despite the above limitations, the model reproduces the order of magnitude of membrane conductivity and some of the observed experimental trends by using an intuitive microscopic picture that captures the essentials of the transport mechanism.

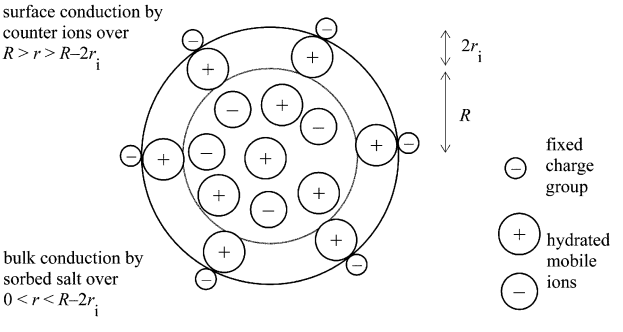

Fig. 1 Schematic view of the pore cross section. The negative charges attached to the pore surface are the fixed charge groups. The pore center is filled by an electroneutral solution because the fixed charges are assumed to be effectively neutralized by the counterions in the surface region. The inner circle denotes the limit of the surface conduction zone, r_i is the effective radius of the hydrated ion, and R is the pore radius.

The membrane conductance can be written as

$$G_m = (A_s/d)k_s^\circ + (A_b/d)k_b^\circ \quad (1)$$

where d is the membrane thickness and k_s° and k_b° are the conductivities of the two regions. The membrane conductivity is defined as

$$k_m = G_m d/A_p = f_s k_s^\circ + f_b k_b^\circ = k_s + k_b \quad (2)$$

where the surface (k_s) and bulk (k_b) contributions to the total membrane conductivity will be referred to as the "surface" and "bulk" conductivities, respectively.

Surface conductivity

The surface conductivity can be evaluated[23] as $k_s = f_s F^2 u_s c_s$, where F is the Faraday constant, u_s is the counterion surface mobility, and c_s is the counterion concentration in the surface region. Since there are no coions in this region and the bulk region is electroneutral, we have that $f_s c_s = X$ (see Fig. 1), where

$$X = 2\sigma_s/FR = 2e/FRl^2 \quad (3)$$

is the membrane fixed charge concentration referred to the pore volume. In eqn. (3), $\sigma_s = e/l^2$ is the charge density on the pore surface, e is the electron charge (absolute value) and l is an average distance between fixed charge groups, assumed to distribute randomly over the membrane.

The calculation of the surface conductivity requires the previous estimation of the surface mobility u_s. In the particular case of perfluorinated ion-exchange membranes, some models for ion hopping have considered the dependence of the activation energy on the membrane water content.[16,24] Extreme membrane dehydration might impact not only on the mobility but also on the effective concentration of counterions in the surface region due to ion pairing with the sulfonic acid groups.[1,4,25] However, we will ignore the above effects and follow a different approach intended to show the relative weights of the surface and bulk contributions to the membrane conductivity. Our analysis could then be regarded as an addition to previous studies focusing on the membrane hydration effects.[1,4,7–9,11,16,26]

We consider the surface conductivity to be given by a series of elementary jumps of the hydrated counterion between neighboring fixed charge groups[16,17] separated by an average distance (see eqn. (3))

$$l = (2/XN_A R)^{1/2} \quad (4)$$

where N_A is the Avogadro number. Each jump is an activated process of energy per ion ΔU_n and pre-exponential frequency $\nu = kT/h$ (a rather crude assumption), where k is the Boltzmann constant, T is the absolute temperature, and h is the Planck constant.[27] The energy ΔU_n should be a function of the hydration radii of the counterion (r_i) and the fixed charge (r_f), the local dielectric constant ε_l characteristic of the water solvation layer between these electrical charges, and the effective jump distance δ. This distance is of the order of the solvent molecular size,[17,28] which is several times smaller than the average distance l between two fixed charge groups, as can be readily shown introducing typical values for the fixed charge concentration in eqn. (4). Indeed, for pore radii in the range $R = 1.5$–3 nm and $X \approx 1$ M, we obtain that $l \approx 1$ nm $> \delta \approx 0.28$ nm for water. Therefore, the counterion needs

a few elementary jumps (and not only one[16]) to proceed from a fixed charge group to a neighboring one. A similar conclusion was obtained for the case of proton transport in polymer electrolyte membranes.[11]

If we assume now that the first jumps $n = 1,2,\ldots$ of the counterion away from the initial fixed charge constitute the rate limiting step for surface transport, the equivalent surface mobility for a series of N jumps is

$$1/u_s = (R_g T/\nu\delta^2)\sum_{n=1}^{N} 1/\exp(-\Delta U_n/kT) \qquad (5)$$

with

$$\Delta U_n = -\frac{e^2}{4\pi\varepsilon_0\varepsilon_l}\left[\frac{1}{r_f + r_i + n\delta} - \frac{1}{r_f + r_i + (n-1)\delta}\right] \qquad (6)$$

where $R_g = N_A k$ is the gas constant and ε_0 is the vacuum permittivity. Note that eqn. (6) is valid only for the first jumps, which are those energetically discouraged.

Eqn. (6) describes a purely Coulombic interaction that ignores changes in the hydration state of the counterion as it moves through the pore. Other Coulombic energy terms different to that of eqn. (6) have been employed previously in the study of the electrostatic interaction between counterions and fixed charges in synthetic[1,16,25] and biological[29] membranes. In particular, the effects that the interaction energy between the counterion and the fixed charge exert on the ionic conductivity have been analyzed by Pourcelly *et al.*,[16] although their approach leads to results quantitatively different from ours, as we show below. Certainly, eqns. (5) and (6) constitute an idealization: the microscopic parameters ε_l and $r_f + r_i$ are not rigorously defined, and the elementary jumps of the counterion may involve not only energy barriers but also entropy changes due to the rearrangement of the hydration shells of the counterion and the fixed group.[30]

Bulk conductivity

The conductivity in the bulk (pore center) region is assumed to be that of the external electrolyte solution[4]

$$k_b^\circ = \Lambda(c)c \qquad (7)$$

where the equivalent conductance $\Lambda(c)$ is a function of the external concentration c.[31] Since the available conductivity data for fixed charge membranes extend up to external concentrations $c \approx 1$ M, ionic conductances are no longer additive due to ion–ion interactions, and expressions for Λ incorporating cross effects[31,32] are needed. We have therefore resorted to the experimental data tabulated by Miller in order to evaluate k_b° (see, in particular, Tables II–IV of ref. 31).

Parameter identification

We will estimate now the parameters introduced in the conductivity equations. The pore radii will be in the range 1.5 nm $< R <$ 4 nm since higher values of R make the contribution of the surface conductivity to the total membrane conductivity negligible while lower values of R can compromise some of the model assumptions. For the thermal frequency at ambient temperature, we obtain $\nu = kT/h \approx 6 \times 10^{12}$ s^{-1} (see ref. 27).

More difficult is to assign values to the sum of the fixed charge and counterion hydration radii $r_f + r_i$, and to the local dielectric constant ε_l in the hydration layer around these charges. Refined models for ion solvation that eliminate in part the need of adjustable parameters for the evaluation of ionic hydration properties have been put forward.[33–35] However, we follow here a more phenomenological approach for the sake of simplicity: we introduce first tentative values for $r_f + r_i$ and ε_l in the model equations, compare the activation energies and diffusion coefficients obtained with experimental data, and assign finally effective values to these parameters. This procedure will prove useful for qualitative purposes.

Although there exist undoubtedly reasonable physical restrictions on the range within the radii may change, the fact is that the "hydrated ion radius" is a fuzzy concept:[29] it is usually the case that estimations based on different experimental properties of electrolyte solutions give significantly different hydrated radii.[22,28,33] Typical ionic radii for naked counterions Li^+, Na^+ and K^+ are 0.068, 0.097 and 0.133 nm, respectively.[36] Also, an effective diameter for the water molecule is 0.28 nm.[29,33] If we consider hydrated ionic radii in the range 0.3–0.4 nm for the above counterions[33] and assume that a solvation layer approximately one water molecule thick is shared between the counterion and the fixed charge (see ref. 36 and references therein), we obtain $r_f + r_i \approx 0.5$–0.6 nm. From Table 8 in chapter 4 of ref. 33, we will tentatively introduce $r_i(Li^+) = 0.382$ nm, $r_i(Na^+) = 0.358$ nm and $r_i(K^+) = 0.331$ nm for the counterion hydrated radii. Also, we take $r_f = 0.15$ nm for the effective fixed charge radius.

For the effective local dielectric constant near the surface of a charged membrane, statistical mechanics models give values significantly lower that the bulk water value,[11,37,38] especially in the vicinity of the fixed charges.[39] In our case, however, ε_l should reflect the solvation properties of the counterion and the fixed charge rather than the dielectric behavior of the water molecules near the polymeric membrane.[26,37–39] Therefore, the local dielectric constant characteristic of the water monolayer between the counterion and the fixed charge group should be much lower than that of bulk water because of the dielectric saturation effect (the water dipoles around a central charge should have a tendency to align in the radial direction of the locally intense electric field).[33,35] A high frequency limit for the dielectric constant assumed in ref. 11 from real refractive index data in their study of proton transfer in polymer electrolyte membranes is $\varepsilon_l = 5$–6. Similar values have also been introduced to simulate the dielectric saturation effects on water molecules near electrodes[28] and to estimate ion solvation properties in the three mode polarization model.[35]

Total membrane conductivity and counterion transport number

From eqns. (2) and (7), the total membrane conductivity is given by

$$k_m = F^2 u_s X + (1 - 2r_i/R)^2 \Lambda(c)c \qquad (8)$$

Also, the counterion transport number in the membrane can be written as

$$t_{+,m} = \frac{k_s + t_{+,b}k_b}{k_s + k_b} \qquad (9)$$

where $t_{+,b}$ is the counterion transport number in the bulk region.

In the case of the Donnan model,[40,41] the membrane conductivity is

$$k_m = \frac{2F^2}{R_g T} D_{+,m}[(X/2)^2 + c^2]^{1/2} \qquad (10)$$

where $D_{+,m} = D_{-,m}$ are the ionic diffusion coefficients in the homogeneous membrane, assumed to be the same for the counterion and the coion for the sake of simplicity. Although this assumption is not quantitatively correct,[1] it does not change the qualitative behavior of eqn. (10) provided that the diffusion coefficients be constant with the external solution concentration.

Results and discussion

Fig. 2 shows the energy change ΔU_n of eqn. (5) in kT units (circles) and the function $\exp(\Delta U_n/kT)$ (triangles) *vs.* the

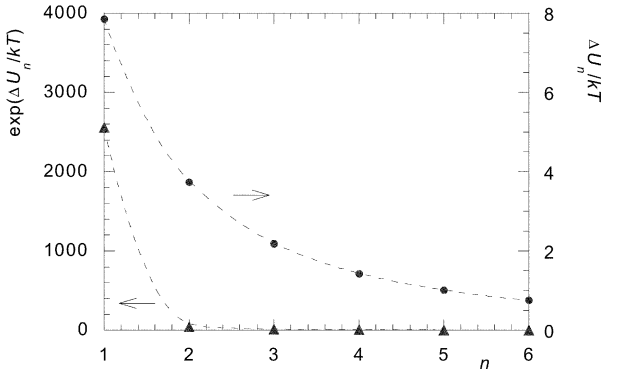

Fig. 2 The energy change ΔU_n in kT units (circles) and the function $\exp(\Delta U_n/kT)$ (triangles) *vs.* the jump number n from the fixed charge with $r_f + r_i(Na^+) = 0.15 + 0.358$ nm, $T = 298.15$ K, $\delta = 0.28$ nm and $\varepsilon_l = 5$.

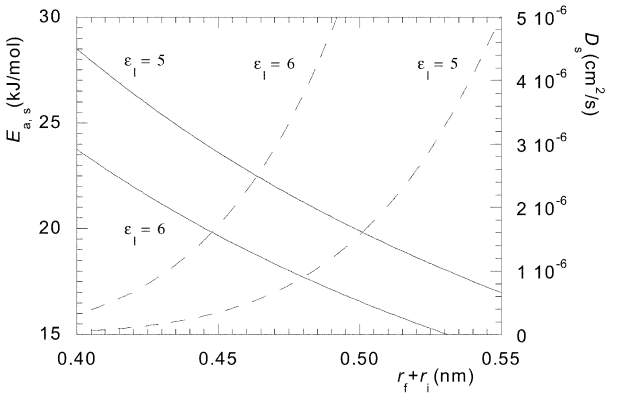

Fig. 3 Activation energy $E_{a,s}$ (continuous curve) and counterion diffusion coefficient D_s (dashed curve) for surface diffusion along the pore *vs.* the sum of the radii $r_f + r_i$. The curves are parametric in the local dielectric constant ε_l. The other parameters as in Fig. 2.

counterion jump number n from the fixed charge with $r_f + r_i(Na^+) = 0.15 + 0.358$ nm, $T = 298.15$ K, $\delta = 0.28$ nm and $\varepsilon_l = 5$. Since $\Delta U_1 \approx 8\ kT > \Delta U_2 \approx 4\ kT$, then $\exp(\Delta U_1/kT) \gg \exp(\Delta U_{n>1}/kT)$ (see Fig. 2) and $\sum_{n=1}^{N} 1/\exp(-\Delta U_n/kT) \approx \exp(\Delta U_1/kT)$ in eqn. (5). Therefore,

$$u_s \approx (\nu\delta^2/R_gT)\exp\left[-\frac{e^2}{4\pi\varepsilon_0\varepsilon_l kT}\frac{\delta}{(r_f + r_i + \delta)(r_f + r_i)}\right] \quad (11)$$

This result means that the first jump of the counterion from the fixed charge is rate limiting for the surface ionic mobility. Therefore,

$$E_{a,s} = \frac{N_A e^2}{4\pi\varepsilon_0\varepsilon_l}\frac{\delta}{(r_f + r_i + \delta)(r_f + r_i)} \quad (12)$$

constitutes a first approximation to the activation energy per mole for surface diffusion. According to eqns. (5) and (11), $E_{a,s}$ should be only weakly dependent on the average distance between fixed charges l because the first jump of the counterion from the fixed charge is rate limiting. (For surface proton transport, however, $E_{a,s}$ is found to increase considerably with l because of the concerted action of the water molecules between the fixed charge groups.[17]) Note finally that the membrane conductivity decreases with increasing l because k_m depends on the fixed charge concentration X, which is proportional to $1/l^2$ in eqn. (3).

Fig. 3 shows the activation energy $E_{a,s}$ and the counterion diffusion coefficient, calculated with the Nernst–Einstein relation[1,23]

$$D_s = R_gTu_s = \nu\delta^2\exp(-E_{a,s}/R_gT) \quad (13)$$

as a function of the sum of the radii $r_f + r_i$. The curves are parametric in the local dielectric constant ε_l. Since ionic diffusion in fixed charge membranes constitutes a complex phenomenon where many effects are simultaneously present,[1,30] it is unlikely that we could obtain accurate values for $E_{a,s}$ and D_s using a simple model incorporating only the Coulombic term of eqn. (6). However, the calculated activation energies for surface diffusion provide interesting clues to microscopic parameters, as it was argued in previous experimental studies.[15,24]

A first inspection of Fig. 3 indicates that the model is very sensitive to the microscopic parameters $r_f + r_i$ and ε_l. The calculated values for D_s are much lower than the typical ionic diffusion coefficients in bulk solutions, $D_b \approx 10^{-5}$ cm^2 s^{-1},[36] except for the curve with $\varepsilon_l = 6$ that gives exceedingly high surface diffusion coefficients. Note also that D_s would take values much lower than those in Fig. 3 if we were to employ the naked instead of the hydrated ion radii in eqn. (13). Counterion diffusion coefficients experimentally obtained in fixed charge membranes are typically in the range 10^{-7}–10^{-6} cm^2 s^{-1}, and should include both the surface and bulk contributions to transport. They cannot then be compared directly to those given by the model because spatial restrictions to ion transport due to the membrane structure not accounted for here could significantly decrease both the surface and bulk transport coefficients in real membranes respect to those obtained here. In membranes with narrow pores, the experimental fact that the counterion diffusion coefficient is found to be significantly lower than the coion diffusion coefficient[1] could reflect the fact that surface diffusion occurs with $D_s \ll D_b$.

The activation energies $E_{a,s} \approx 20$–30 kJ mol^{-1} (curve with $\varepsilon_l = 5$) are higher than the experimental activation energies for diffusion of small ions like Li^+, Na^+ and K^+ in bulk aqueous solutions, $E_{a,b} \approx 12$–15 kJ mol^{-1}.[42] As could be expected, experimental data for fixed charge membranes give intermediate values for the effective activation energy, $E_a \approx 14$–24 kJ mol^{-1},[14,43] since both surface and bulk diffusion should be simultaneously present in narrow pores. Note that if we assume $r_i \approx 0.3$–0.4 nm for the hydrated radii of Li^+, Na^+, and K^+,[33] reasonable activation energies can be obtained with $r_f \approx 0.15$ nm and $r_f + r_i \approx 0.5$ nm for $\varepsilon_l = 5$, which could be a realistic value for the sum of hydrated radii if a water layer one molecule thick existed between the fixed charge group and the counterion.[36] It should be noted that previous theoretical estimations[16] for the electrostatic interaction between the fixed charge and the counterion led to activation energies for surface diffusion lower than those in Fig. 3.

Experimental data of perfluorosulfonic membranes with narrow pores and high fixed charge concentrations have found that $E_a(K^+) > E_a(Na^+)$ by 1 kJ mol^{-1} approximately[24] despite the fact that $E_{a,b}(K^+) < E_{a,b}(Na^+)$ for bulk diffusion.[42] It is tempting to analyze this finding using the results in Fig. 3 (curve with $\varepsilon_l = 5$). If we introduce $r_f \approx 0.15$ nm together with the respective hydrated counterion radii for K^+ and Na^+[33] in the sum $r_f + r_i$, we obtain indeed that $E_{a,s}(K^+) > E_{a,s}(Na^+)$ (see Fig. 3).

For some divalent counterions, it might be argued that the moderate increase in the hydrated radii[33] could not compensate for the twofold increase in the ionic charge number (see eqn. (12)). In this case, the surface diffusion coefficients D_s for divalent counterions would be significantly lower than those of monovalent counterions. Previous studies on ionic transport through fixed charge membranes have found significant differences between between monovalent, divalent and trivalent cations,[15,16,36] although the effects were not so dramatic as eqns. (12)–(13) might suggest. This could reflect a serious limitation of these equations but also the fact that experimental membrane conductivities include both the surface and bulk contributions while eqn. (13) applies only to k_s.

Interestingly enough, if we introduce $r_f + r_i \approx 0.532$ nm for Li^+ and $r_f + r_i \approx 0.481$ nm for K^+ in eqn. (6) according to the above estimations, then $D_s(Li^+)/D_s(K^+) > 1$ (see Fig. 3) despite the fact that $D_b(Li^+)/D_b(K^+) < 1$ over a broad concentration range.[44] Apparently, similar reversals for the counterion diffusion coefficients and mobilities have been observed experimentally.[15,24] In the present model, this effect arises from the influence of counterion hydration on the different transport mechanisms operating in surface and bulk diffusion. Speaking loosely, the smaller naked counterion Li^+ is more hydrated than the larger naked counterion K^+.[29,33] Let us assume now, contrary to the cases of some low water content membranes[1] and the extremely narrow ionic channels present in biological membranes,[29] that surface diffusion occurred without significant counterion dehydration. Then, the strong electrostatic interaction of K^+ with the fixed charge groups would lead to a surface mobility lower than that of Li^+ whose interaction should be considerably weaker because of its higher effective radius (see eqn. (6)).[15,34,36] For bulk diffusion in water, however, the opposite effect occurs: the highly hydrated Li^+ has a bulk mobility lower than that of K^+ because of the hydrodynamic friction with the solvent.[1,33]

Fig. 4 shows the membrane conductivity k_m *vs.* the solution concentration c. The continuous curve has been calculated using eqn. (8) with $r_i(Na^+) = 0.358$ nm, $r_f = 0.15$ nm, $c_s = 1$ M ($X = 0.65$ M for $R = 1.75$ nm), and $\varepsilon_l = 5$. The dashed curve corresponds to eqn. (10) for the Donnan conductivity with $X = 1$ M and $D_{+,m} = D_{-,m} = 2D_s$ to show clearly the different curve shapes. The dotted curve is the experimental conductivity of a bulk NaCl aqueous solution,[31] which is much higher than k_m at high solution concentrations, as it is observed experimentally.[4,45,46] The theoretical conductivities are of the order of magnitude of the experimental values,[4,10,14,43,45–47] although some qualitative discrepancies with experiments should be mentioned. The Donnan conductivity is concave upwards (assuming that the ionic diffusion coefficients do not change significantly with the external solution concentration) while the two region membrane conductivity $k_m = k_s + k_b$ is concave downwards because of the experimental behavior of k_b. In agreement with the two region model, experimental conductivities show concave downwards curves[4,10,14,43,45–47] but with a drop of k_m for small values of c that is missing in the results of Fig. 4. Presumably, the Donnan and the two region models give finite, non-zero conductivities in the limit of low c because they assume erroneously that the counterions compensating for the fixed charge concentration are mobile even at $c = 0$, ignoring the effect of the diffusion boundary layers flanking the membrane, which are the reservoirs of mobile ions. Note also that the details of membrane structure (including possible inhomogeneity effects[48]) are not considered in the model. It is conceivable that spatial restrictions due to the membrane structure give experimental surface conductivities lower that those calculated here. If this were the case, decreasing c would produce a marked decrease of $k_m \approx k_b$ because of the rapid increase of the solution conductivity curve with c in Fig. 4. Finally, the experimental tendency to saturation shown by some experimental conductivity curves at high external concentrations might reflect both membrane structural effects not accounted for here as well as the invalidity of our assumption concerning the existence of an electroneutral region in the pore center for very narrow membrane pores. These limitations of the two theoretical models considered here should be kept in mind when attempting to use them in the analysis of experimental data.

Fig. 5 shows the counterion transport number $t_{+,m}$ *vs.* the solution concentration c. The continuous curve has been calculated using eqn. (9) for the surface and bulk contributions with the same parameters of Fig. 4 and $t_{+,b} = 0.5$. The dashed curve corresponds to the transport number given by the Donnan model[1,6] with $D_{+,m} = D_{-,m} = 2 \times 10^{-5}$ cm^2 s^{-1}. The curves are parametric in the fixed charge concentration X. For $c < X$, the counterion transport number calculated with the homogeneous Donnan model is concave downwards (if the ionic diffusion coefficients do not change significantly with the external solution concentration) while that calculated with eqn. (9) is concave upwards. Experimental data show usually this behavior (see in particular Fig. 4 of ref. 6 and references therein), with transport numbers significantly lower than those predicted by the homogeneous membrane model.[6,48,49] These findings are in qualitative agreement with the predictions of the model in Fig. 5. As it could be expected, Figs. 4 and 5 show that on increasing c the electrolyte uptake from the solution incorporates both counterions and coions to the bulk region, and this causes the membrane conductivity to increase and the counterion selectivity to decrease.

Fig. 6 shows the membrane conductivity k_m *vs.* the solution concentration c obtained by the numerical solution of a modified Poisson–Boltzmann equation extended to include the finite size of the mobile ions. This equation is solved together with the Nernst–Planck flux equations and the Navier–Stokes equation[50] for a cylindrical pore containing a surface charge density σ_s adjusted to give $X = 0.5$ M (constant) for each pore radius R (see eqn. (3)). Other parameters are $r_i(Na^+) = 0.358$ nm

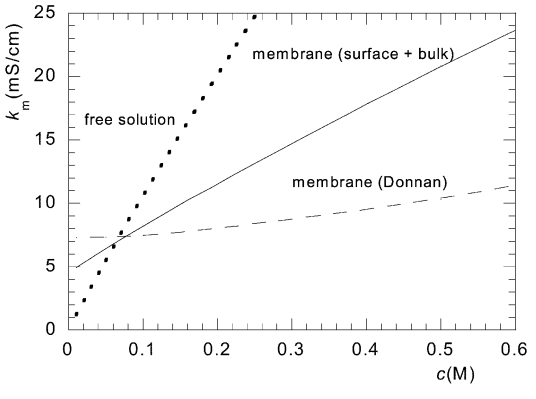

Fig. 4 Membrane conductivity k_m *vs.* the solution concentration c. The continuous curve has been calculated using eqn. (8) for the surface and bulk contributions with $r_i(Na^+) = 0.358$ nm, $r_f = 0.15$ nm, $R = 1.75$ nm, $c_s = 1$ M ($X = 0.65$ M) and $\varepsilon_l = 5$. The dashed curve corresponds to eqn. (10) for the Donnan conductivity with $D_{+,m} = D_{-,m} = 2D_s$ and $X = 1$ M. The dotted curve is the conductivity of a bulk NaCl aqueous solution.[31]

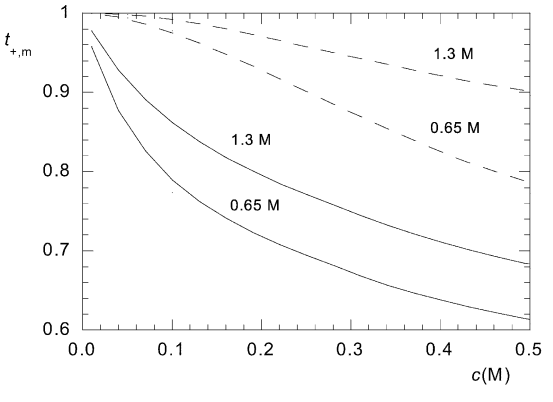

Fig. 5 Counterion transport number $t_{+,m}$ *vs.* the solution concentration c. The continuous curve has been calculated using eqn. (9) for the surface and bulk contributions with the same parameters of Fig. 4 and $t_{+,b} = 0.5$. The dashed curve corresponds to the Donnan model[6] with $D_{+,m} = D_{-,m} = 2 \times 10^{-5}$ cm^2 s^{-1}. The curves are parametric in the fixed charge concentration X ($c_s = 1$ M gives $X = 0.65$ M and $c_s = 2$ M gives $X = 1.3$ M for $R = 1.75$ nm).

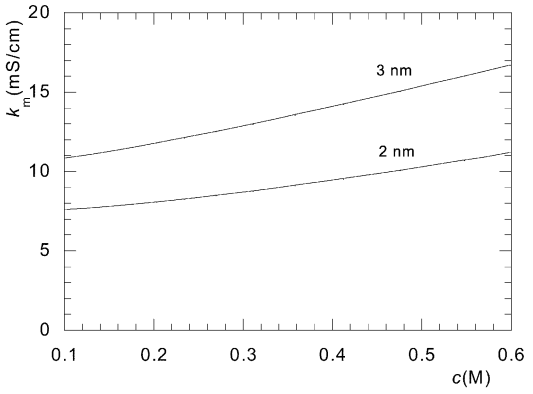

Fig. 6 Membrane conductivity k_m *vs.* the solution concentration c obtained by the numerical solution of the Poisson–Boltzmann equation extended to finite size ions[50] for cylindrical pores of radius 2 and 3 nm. The surface charge density is varied to keep $X = 0.5$ M in both cases (see eqn. (3)). Other parameters are $\varepsilon_r = 30$ for the dielectric constant of the water confined to the pore and $r_i(Na^+) = 0.358$ nm. The ionic diffusion coefficients are $D_{+,m} = D_{-,m} = D\mathcal{F}(r_i/R)$ with $D = 10^{-5}$ cm^2 s^{-1}. $\mathcal{F}(r_i/R)$ is the Renkin function accounting for ion size.[50]

and $\varepsilon_r = 30$ for the dielectric constant of the water confined to the pore. The ionic diffusion coefficients are $D_{+,m} = D_{-,m} = D\mathcal{F}(r_i/R)$ where $D = 10^{-5}$ cm^2 s^{-1} and $\mathcal{F}(r_i/R)$ is the Renkin function for the ion size correction.[50] As in the case of the homogeneous Donnan model, the continuous model based on the Poisson–Boltzmann equation gives concave upwards curves for k_m when the ionic diffusion coefficients are assumed to be constant, contrary to many experiments.[4,43,46]

Fig. 7 shows the values of k_m *vs.* c for several pore radii R at constant fixed charge concentration. The other parameters as in Fig. 4. Compare the downwards concavity of the curves in Fig. 7 with the upwards concavity of the curves in Fig. 6. Experimental studies have considered the dependence of the membrane conductivity on the water content of the membrane (in particular, on the hydration of the counterions in the surface region and the fixed charges).[4,7,16,24] Although we have not addressed these effects here, we could understand qualitatively now the role of membrane hydration from the results of Figs. 3 and 7. It has been suggested that the activation energy barrier for surface diffusion depends on the hydration of the counterion and the fixed charge.[16] This follows from Fig. 3 if we assume that dehydration decreases the sum of radii $r_f + r_i$, as suggested previously.[16] Indeed, decreasing the effective distance for the Coulombic interaction leads to higher activation energies for surface diffusion in Fig. 3 (see eqn. (12)). However,

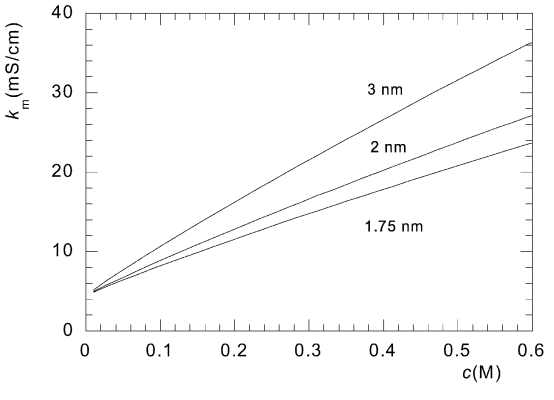

Fig. 7 Membrane conductivity k_m *vs.* the solution concentration c for several pore radii R. The other parameters as in Fig. 4.

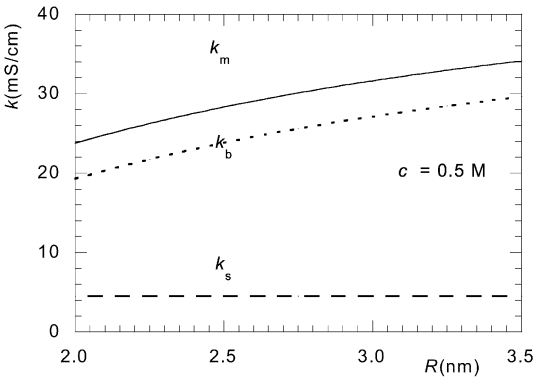

Fig. 8 The surface (dashed curve) and bulk (dotted curve) contributions to the total membrane conductivity (full curve) *vs.* the pore radius for $c = 0.5$ M giving $k_b^\circ = 46.81$ mS cm^{-1} in the case of a NaCl aqueous solution.[31] The other parameters as in Fig. 4.

solvation energies are so high for small ions[28,29,33] that membrane dehydration must decrease also the free water content in the bulk region where the electrolyte is sorbed[1] squeezing the pore to lower radii. This causes a decrease of the bulk region size, which is the most conductive one at high external solution concentrations. The drop in the conductivity observed experimentally at low membrane water content[4,7,15] could therefore be understood from Fig. 7, that shows the significant decrease of k_m with decreasing R for high c.

Fig. 8 shows the surface (dashed curve) and bulk (dotted curve) contributions to the total membrane conductivity (full curve) *vs.* the pore radius for a solution concentration $c = 0.5$ M at constant fixed charge concentration (and then constant surface conductivity, according to eqn. (8)). This gives $k_b^\circ = 46.81$ mS cm^{-1} for the NaCl aqueous solution considered.[31] The other parameters as in Fig. 4. The theoretical predictions show that $k_b \gg k_s$ for this relatively high external solution concentration provided that the pore radius does not assume extremely low values. Fig. 9 shows also the surface and bulk contributions to the total membrane conductivity *vs.* the pore radius but now for a solution concentration $c = 0.1$ M. This gives $k_b^\circ = 10.67$ mS cm^{-1} for the NaCl aqueous solution considered.[31] The other parameters as in Fig. 4. Contrary to the case of Fig. 8, k_b and k_s take now similar values. It can be concluded from Figs. 8 and 9 that the surface contribution to the membrane conductivity can be significant for narrow pores at low enough external solution concentrations, in qualitative agreement with the experimental findings cited in ref. 51.

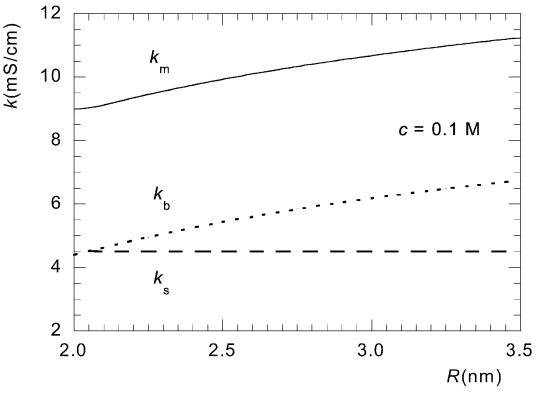

Fig. 9 The surface (dashed curve) and bulk (dotted curve) contributions to the total membrane conductivity (full curve) *vs.* the pore radius for $c = 0.1$ M giving $k_b^\circ = 10.67$ mS cm^{-1} in the case of a NaCl aqueous solution.[31] The other parameters as in Fig. 4.

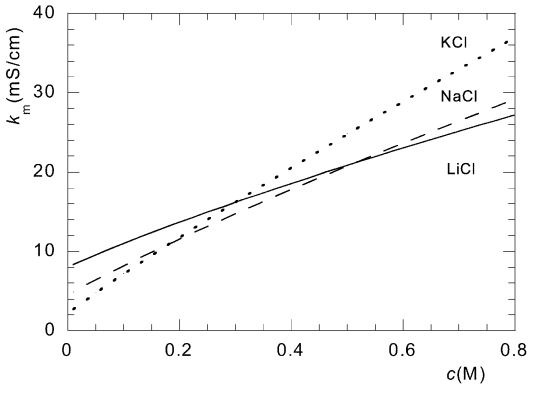

Fig. 10 Membrane conductivity k_m *vs.* the solution concentration c for LiCl (full curve), NaCl (dashed curve) and KCl (dotted curve) aqueous solutions with $r_i(Li^+) = 0.382$ nm, $r_i(Na^+) = 0.358$ nm, and $r_i(K^+) = 0.331$ nm. The bulk conductivity k_f° was obtained from tabulated data for each electrolyte solution.[31] The other parameters as in Fig. 4.

Fig. 10 shows finally the membrane conductivity *vs.* the solution concentration c for the electrolytes LiCl (full curve), NaCl (dashed curve) and KCl (dotted curve) in aqueous solution. The membrane parameters are the same as in Fig. 4. As it was commented in Fig. 4, the experimental curves[4,10,46] tend to increase more rapidly with c than do the theoretical curves at low external solution concentrations. At high concentrations the series $k_b(LiCl) < k_b(NaCl) < k_b(KCl)$ dictates the behavior of k_m with c despite the fact that $k_s(Li) > k_s(Na) > k_s(K)$ regardless of c because the assumed hydrated radii follow the series $r_i(Li^+) = 0.382$ nm $> r_i(Na^+) = 0.358$ nm $> r_i(K^+) = 0.331$ nm.[33] The above trend is reversed for low enough concentrations where the dominance of the surface conductivity over the low bulk conductivity gives now $k_m(LiCl) > k_m(NaCl) > k_m(KCl)$. Therefore, for narrow pores and low external solution concentrations the membrane conductivity series for the three electrolytes can be reversed respect to the bulk solution case. This reversal could be confirmed in previous experimental findings[15,24] where the membrane conductivity was correlated to the counterion hydration state. Eqns. (8) and (11) together with the results of Figs. 3 and 10 provide an explanation for the above effect because when the effective distance of the interaction $r_f + r_i$ increases (due to higher counterion hydration) k_m also increases due to the lower Coulombic interaction between mobile and fixed charges.[24]

In conclusion, although the model showed some inconsistencies when compared with experiments, presumably because of the complex nature of the ionic transport phenomena in fixed charge membranes and the simplifications introduced, we believe that the results provide a qualitative understanding of the surface and bulk contributions to the total ionic conductivity of the membrane. Although the surface transport occurs with a higher activation energy than the bulk transport (and then with a lower transport coefficient, see Fig. 3), this mechanism can be significant for narrow pores at external solution concentrations lower than the fixed charge concentration. It is also in this limit that the membrane can discriminate efficiently not only the counterion from the coion (see Fig. 5) but also one particular counterion from other counterions having the same charge number but different hydration properties (see Fig. 10). This ionic selectivity arises from the sensitivity of the activation energy for surface transport to the values of a reduced number of microscopic parameters. Unfortunately, the highly idealized microscopic model considered here together with the uncertain nature of the above parameters make our results of limited use for the quantitative interpretation of experimental data. This would require use of modern molecular approaches for the independent estimation of the solvation and Coulombic energies involved in surface transport together with knowledge of the structural properties of each membrane.

Acknowledgements

Financial support from the CICYT and FEDER, Project No. MAT2002-00646 is gratefully acknowledged. The authors thank also Javier Cervera for solving numerically the Poisson–Boltzmann equation in the case of finite size ions.

References

1 F. Helfferich, *Ion Exchange*, McGraw-Hill, NY, 1962.
2 Y. Kobatake and N. Kamo, *Prog. Polym. Sci. Jpn.*, 1973, **5**, 257.
3 P. Meares, *J. Membr. Sci.*, 1981, **8**, 295.
4 N. P. Berezina, N. A. Kononenko and O. A. Demina, *Elektrokhimiya*, 1996, **32**, 173Russ. J. Electrochem.1996, **32**, 154.
5 V. I. Zabolotsky and V. V. Nikonenko, *J. Membr. Sci.*, 1993, **79**, 181.
6 K. Kontturi, S. Mafé, J. A. Manzanares, L. Murtomäki and P. Viinikka, *Electrochim. Acta*, 1994, **39**, 883.
7 T. Okada, G. Xie, O. Gorseth, S. Kjelstrup, N. Nakamura and T. Arimura, *Electrochim. Acta*, 1998, **43**, 3741.
8 M. W. Verbrugge and R. F. Hill, *J. Electrochem. Soc.*, 1990, **137**, 893.
9 N. P. Gnusin, N. P. Berezina, O. A. Demina and N. A. Kononenko, *Elektrokhimiya*, 1992, **28**, 1050Sov. Electrochem.1992, **28**, 873.
10 N. P. Berezina, N. Gnusin, O. Dyomina and S. Timofeyev, *J. Membr. Sci.*, 1994, **86**, 207.
11 M. Eikerling and A. A. Kornyshev, *J. Electroanal. Chem.*, 2001, **502**, 1.
12 N. Lakshminarayanaiah, *Equations of Membrane Biophysics*, Academic Press, NY, 1984.
13 D. Li, in *Encyclopedia of Surface and Colloid Science*, ed. A. Hubbard, Marcel Dekker, NY, 2002, p. 3167.
14 T. Okada, G. Xie and M. Meeg, *Electrochim. Acta*, 1998, **43**, 2141.
15 T. Okada, H. Satou, M. Okuno and M. Yuasa, *J. Phys. Chem. B*, 2002, **106**, 1267.
16 G. Pourcelly, A. Oikonomou, C. Gavach and H. D. Hurwitz, *J. Electroanal. Chem.*, 1990, **287**, 43.
17 M. Eikerling, A. A. Kornyshev, A. M. Kuznetsov, J. Ulstrup and S. Walbran, *J. Phys. Chem. B*, 2001, **105**, 3646.
18 W. Y. Hsu, J. R. Barkley and P. Meakin, *Macromolecules*, 1980, **13**, 198.
19 A. Eisenberg and J.-S. Kim, *Introduction to Ionomers*, Wiley, NY, 1998.
20 W. J. McHardy, P. Meares, A. H. Sutton and J. F. Thain, *J. Colloid Interface Sci.*, 1969, **9**, 116.
21 R. Tandon and P. N. Pintauro, *J. Membr. Sci.*, 1997, **136**, 207.
22 Y. Marcus, *Ion Properties*, Marcel Dekker, NY, 1997.
23 G. Pourcelly, P. Sistat, A. Chapotot, C. Gavach and V. Nikonenko, *J. Membr. Sci.*, 1996, **110**, 69.
24 C. Gavach, G. Pamboutzoglou, M. Nedyalkov and G. Pourcelly, *J. Membr. Sci.*, 1989, **45**, 37.
25 K. A. Mauritz and A. J. Hopfinger, in *Modern Aspects of Electrochemistry*, ed. J. O'M Bockris, B. E. Conway and R. E. White, Plenum, New York, 1982, vol. 14, p. 425.
26 S. J. Paddison and R. Paul, *Phys. Chem. Chem. Phys.*, 2002, **4**, 1158.
27 T. L. Hill, *An Introduction to Statistical Thermodynamics*, Dover, New York, 1985.
28 J. O'M. Bockris and A. K. N. Reddy, *Modern Electrochemistry*, Plenum, NY, 2000.
29 B. Hille, *Ionic Channels of Excitable Membranes*, Sinauer, Sunderland, 1992.
30 S. F. Timashev, *Physical Chemistry of Membrane Processes*, Ellis Horwood, NY, 1991.
31 D. G. Miller, *J. Phys. Chem.*, 1966, **70**, 2639.
32 D. G. Miller, *Faraday Discuss. Chem. Soc.*, 1978, **66**, 295.
33 B. E. Conway, *Ionic Hydration in Chemistry and Biophysics*, Elsevier, Amsterdam, 1985.
34 J. R. Bontha and P. N. Pintauro, *Chem. Eng. Sci.*, 1994, **49**, 3835.

35 V. S. Markin and A. G. Volkov, *Electrochim. Acta.*, 1989, **34**, 93.
36 T. Xue, R. B. Longwell and K. Osseo-Asare, *J. Membr. Sci.*, 1991, **58**, 175.
37 M. Schlenkrich, K. Nicklas, J. Brickmann and P. Bopp, *Ber. Bunsen-Ges. Phys. Chem.*, 1990, **94**, 133.
38 R. Paul and S. J. Paddison, *J. Chem. Phys.*, 2001, **115**, 7762.
39 K. Lebedev, S. Mafé, A. Alcaraz and P. Ramirez, *Chem. Phys. Lett.*, 2000, **326**, 87.
40 R. P. Buck, *J. Membr. Sci.*, 1984, **17**, 1.
41 K. Asaka, *Maku*, 1989, **14**, 54.
42 J. P. Gong, N. Komatsu, T. Nitta and Y. Osada, *J. Phys. Chem. B*, 1997, **101**, 740.
43 A. Lehmani, P. Turq, M. Périé, J. Périé and J.-P. Simonin, *J. Electroanal. Chem.*, 1997, **428**, 81.
44 R. A. Robinson and R. H. Stokes, *Electrolyte Solutions*, Butterworth, London, 1959.
45 A. Elattar, A. Elmidaoui, N. Pismenskaia, C. Gavach and G. Pourcelly, *J. Membr. Sci.*, 1998, **143**, 249.
46 L. Dammak, R. Lteif, G. Bulvestre, G. Pourcelly and B. Auclair, *Electrochim. Acta*, 2001, **46**, 451.
47 A. Narebska, S. Köter and W. Kujawski, *J. Membr. Sci.*, 1985, **25**, 153.
48 J. H. Petropoulos, *J. Membr. Sci.*, 1990, **52**, 305.
49 E. H. Cwirko and R. G. Carbonell, *J. Membr. Sci.*, 1992, **67**, 211.
50 J. Cervera, J. A. Manzanares and S. Mafé, *J. Membr. Sci.*, 2001, **191**, 179.
51 C. L. Bashford, G. M. Alder and Ch. Pasternak, *Biophys. J.*, 2002, **82**, 2032.